Supporting Information for: Optical Excitation of a Nanoparticle Cu/p-NiO Photocathode Improves Reaction Selectivity for CO_2 Reduction in Aqueous Electrolytes

*Joseph S. DuChene[†§], Giulia Tagliabue[†§], Alex J. Welch[†§], Xueqian Li[†§], Wen-Hui Cheng[†§], and Harry A. Atwater[†§]**

[†]Thomas J. Watson Laboratory of Applied Physics and [§]Joint Center for Artificial Photosynthesis, California Institute of Technology, Pasadena, California 91125 United States.

Methods

Synthesis of p-NiO films and plasmonic Cu/p-NiO photocathodes

Plasmonic Cu/p-NiO photocathodes were constructed via electron beam physical vapor deposition. The p-type NiO (p-NiO) films were first synthesized on fluorine-doped tin oxide (FTO) glass substrates by depositing Ni metal at a rate of 0.25 Å s^{-1} under flowing O_2 gas at 6 sccm. After deposition of a 60 nm-thick NiO film on the FTO substrate, the film was annealed in ambient air at 300 °C for 1 h to ensure complete conversion to the desired p-NiO phase. After the heat treatment, 3 nm of Cu was then deposited onto the p-NiO surface using electron-beam physical vapor deposition at a base pressure of ca. 1 x 10^{-7} torr and a deposition rate of 1.0 Å s^{-1}.

Optical characterization of materials

The optical properties of the Cu nanoparticles and the bare p-NiO films were characterized via UV-Vis absorption spectroscopy (Varian Cary UV-50) both “as-deposited” (prior to any electrochemical treatment) and after electrochemical reduction with cyclic voltammetry. The Cu nanoparticles were also deposited onto bare FTO glass substrates in the absence of the underlying p-NiO film. The background absorption of bare FTO glass was used as the reference standard for all samples. The films were first characterized in their as-deposited state and then the Cu nanoparticles were reduced by performing successive cyclic voltammetry scans from 0.8 V_{RHE} to −0.6 V_{RHE} (V vs. RHE) at a scan rate of 50 mV s^{-1} until the reductive wave around 0.7 V_{RHE} due to copper oxide reduction was no longer observable. The sample was then removed from the electrolyte, blown dry with a stream of N_2, and then immediately loaded into the

spectrophotometer to obtain the optical properties of the reduced form of Cu presumably present upon actual electrochemical CO_2 reduction conditions.

Photoelectrochemical characterization of bare p-NiO and plasmonic Cu/p-NiO photocathodes

All glassware was cleaned with aqua regia (3:1 HCl:HNO_3) before use to remove any trace metal ions. All electrochemical experiments were performed in a three-electrode configuration with the p-NiO or Cu/p-NiO photocathode as the working electrode, a Pt wire mesh counter electrode, and a saturated calomel reference (SCE) electrode all immersed in 50 mM K_2CO_3 electrolyte. The electrolyte was sparged with CO_2 gas prior to measurements to remove dissolved O_2 from the solution and experiments were conducted under a CO_2 blanket. All electrode potentials were converted to the reversible hydrogen electrode (RHE) scale through the following equation: E vs. RHE = E vs. SCE + (0.059 V pH^{-1} x pH) + 0.2401 V. Electrochemical impedance spectroscopy was performed under dark conditions with a 20 mV sinusoidal amplitude across a range of frequencies (0.1–50 kHz). At higher frequencies (1-10 kHz) used for analysis, the data can be reasonably represented by a resistor in series with a capacitor.[1]

Incident photon-to-charge conversion efficiency [IPCE(λ)] measurements of the plasmonic Cu/p-NiO and bare p-NiO photocathodes was acquired using a series of high-power LEDs (Thor Labs, Inc.) with central wavelengths of 415 nm (FWHM 14 nm), 450 nm (FWHM 18 nm), 505 nm (FWHM 30 nm), 565 nm (FWHM 104 nm), and 780 nm (FWHM 30 nm). The LED power was adjusted to ensure that the same photon flux was incident on the sample for all wavelengths during the IPCE measurement. The IPCE was determined by collecting the photocurrent from each device under illumination while poised at an applied potential of E_{appl} = −0.2 V_{RHE}. The IPCE was calculated according to the following expression:

$$IPCE(\lambda) = \frac{J_{ph}\left(\mathrm{A}/_{\mathrm{cm}^2}\right)}{I_0\left(\mathrm{W}/_{\mathrm{cm}^2}\right)} \times \frac{1240}{\lambda(\mathrm{nm})} \times 100\%$$

Open-circuit photovoltage measurements were performed in a quiescent solution after allowing 2-3 hours for Fermi level equilibration between the working electrode and the electrolyte to achieve a steady baseline open-circuit voltage prior to illumination with a 565 nm LED at full power (160 mW cm^{-2}).

Photoelectrochemical experiments for plasmon-driven CO_2 reduction

The CO_2 reduction reaction (CO_2RR) was conducted in a three-electrode configuration with Cu/p-NiO or bare p-NiO cathode as the working electrode, Pt wire gauze as the counter electrode, and a leakless Ag/AgCl electrode as the reference electrode. All photoelectrochemical experiments were conducted within a custom-built, airtight cell equipped with a quartz window, as described previously.[1] The photoelectrochemical experiments were performed in 50 mM K_2CO_3 electrolyte (pH 7) that was fully saturated with CO_2 by vigorous bubbling of the cathode and anode compartments for 1 h before commencing with the

experiment. The internal solution resistance was estimated from an impedance measurement, which routinely indicated a solution resistance of around 50 Ohm. No *iR* correction was applied to any of the electrochemical experiments. Prior to electrocatalysis, a Cu/p-NiO film was prepared by performing five successive linear sweep voltammograms from 0.8 V_{RHE} to −0.6 V_{RHE} (V vs. RHE) at a scan rate of 50 mV s^{-1} until no reductive wave was observable in the voltammogram, indicating complete reduction of any residual copper oxides.

After this initial electrochemical preparation of the Cu/p-NiO photocathode, the device was then held potentiostatically at the indicated applied potential (starting from −0.7 V_{RHE}) under dark conditions for 2 h. The experiments were performed under continuous flow conditions at a CO_2 flow rate of 5 sccm in a flow-cell device with periodic sampling of the reactor headspace every 15 min over the course of the 2 h reaction with a gas chromatograph. The gas chromatograph (SRI-8610) was equipped with a Hayesep D column and a Molsieve 5A column using N_2 as carrier gas. The gaseous products were detected using a thermal conductivity detector (TCD) and flame ionization detector (FID) equipped with a methanizer. The average of gas-phase products was determined from seven data points taken over 2 h, discarding the first GC measurement that was acquired prior to steady-state conditions. Quantitative analysis of gaseous products was based on calibration with several gas standards over many orders of magnitude in concentration. After each electrolysis experiment at a given applied potential, liquid products were collected from the cathode and anode compartments at the end of the 2 h electrolysis experiment and analyzed by high-pressure liquid chromatography (Thermo Fischer Dionex UltiMate 3000).

After electrolyte sampling, the electrochemical cell was flushed with H_2O three times and then re-filled with fresh 50 mM K_2CO_3 electrolyte and scanned from 0.8 V_{RHE} to −0.6 V_{RHE} at a scan rate of 50 mV s^{-1} to ensure no copper oxides were formed on the device upon brief exposure to ambient air. The new electrolyte was then purged with CO_2 at a flow rate of 15 sccm for 5-10 min to saturate the solution with CO_2, as evidenced by a similar CO_2 flow rate measured before and after the electrochemical cell with mass flow controllers (Alicat Scientific). Then the CO_2 flow rate was returned to 5 sccm before the light was switched on to repeat electrolysis at the same applied potential as before. Visible-light irradiation (λ = 565 ± 52 nm FWHM) with a high-power LED was incident on the sample through the quartz window at an incident power of I_0 = 160 mW cm^{-2} (measured at the quartz window). Photoelectrolysis experiments were conducted with a thermocouple inserted into the cell to monitor the solution temperature during the 2 h experiment. We observed a modest increase in solution temperature from around 25 °C at the start of the experiment to eventually stabilize around 29 °C after 2 h of photoelectrolysis (Figure S9).

This electrolysis procedure was repeated (dark/light) at each applied potential from −0.7 V_{RHE} to −0.9 V_{RHE} and was performed starting from −0.7 V_{RHE} before moving to more negative potentials. All catalytic experiments at a given applied potential were repeated in triplicate on fresh Cu/p-NiO photocathodes.

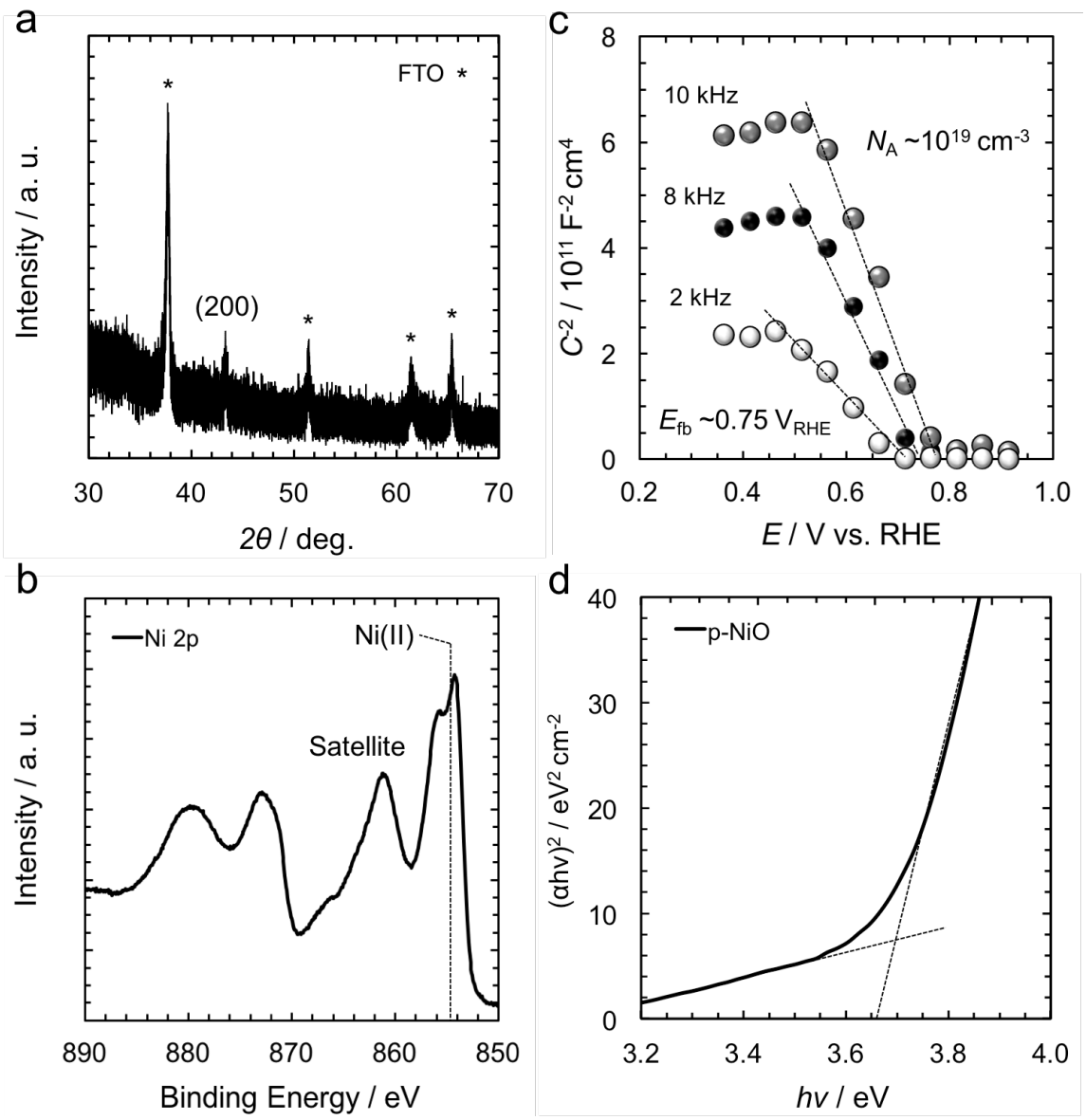

Figure S1. Materials characterization of p-type NiO films. (**a**) X-ray diffraction pattern from NiO film on FTO glass showing the characteristic (200) peak of NiO. All other peaks can be attributed to the underlying FTO substrate. (**b**) X-ray photoelectron spectroscopy high-resolution scan of the Ni 2p region, showing the characteristic binding energies and satellite features of NiO. (**c**) Mott-Schottky plot obtained from NiO films on FTO glass substrate, which shows a negative slope indicative of p-type conductivity. From a linear fit of these data, the flat-band potential (E_{fb}) is estimated to be ca. 0.75 V_{RHE} (Volts vs. RHE) with an acceptor concentration of ca. 1 x 10^{19} cm^{-3}. (**d**) Tauc plot of the NiO film showing a band gap of around 3.7 eV. All these data indicate material properties consistent with previous literature reports of p-type NiO thin films.[1]

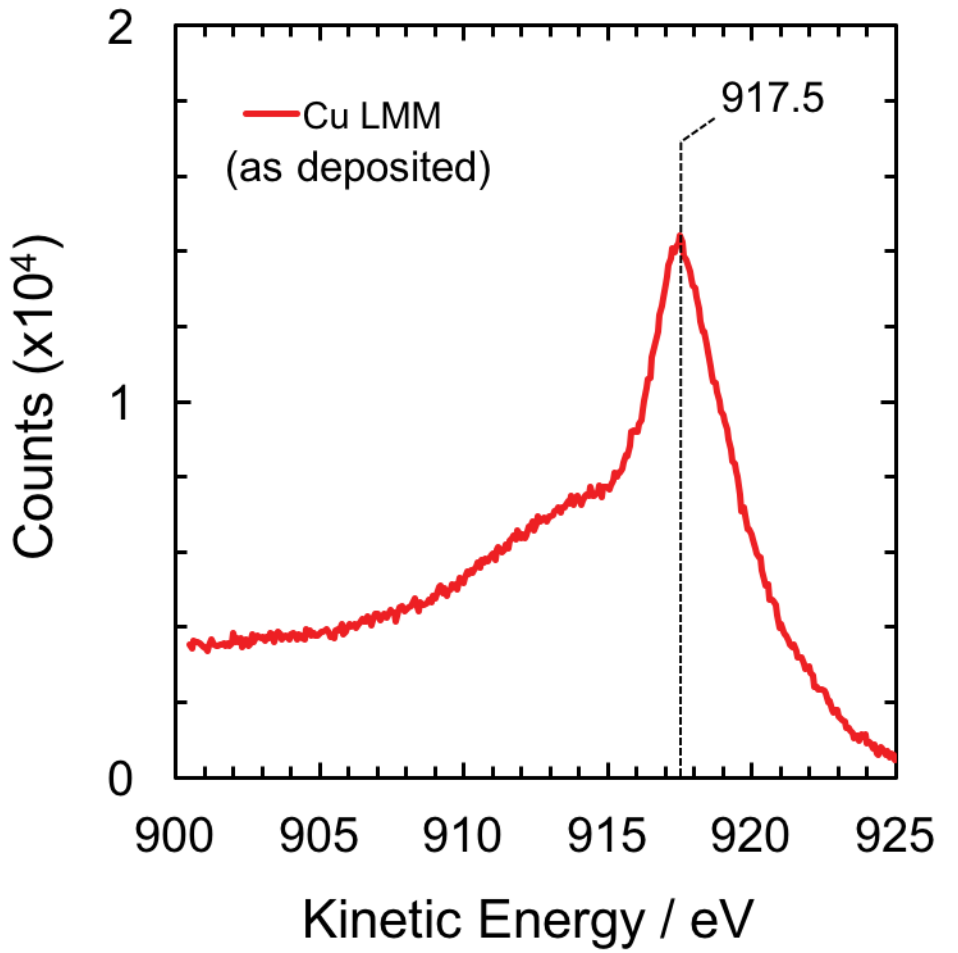

Figure S2. XPS of Cu LMM region from Cu/p-NiO photocathodes prior to electrochemical reduction. The spectral profile and the peak in kinetic energy at 917.5 eV is consistent with the CuO phase.

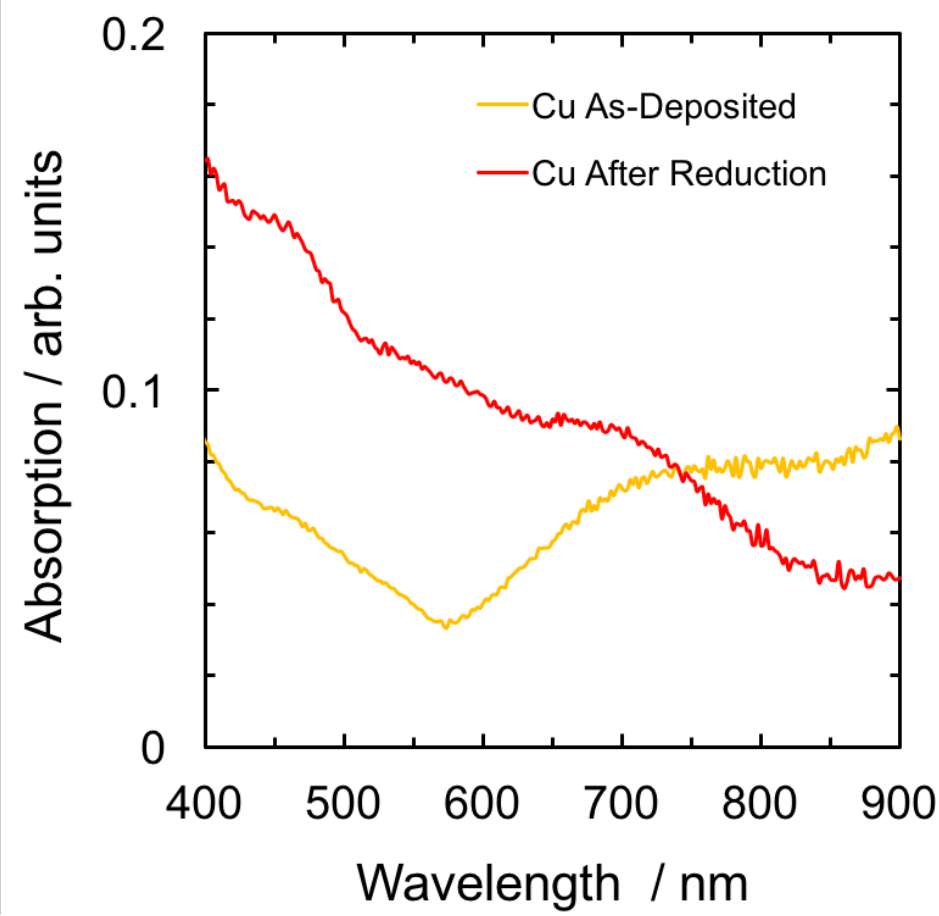

Figure S3. Absorption spectra of Cu nanoparticles on bare FTO substrates without the underlying p-NiO film. The absorption spectra of the as-deposited Cu nanoparticles (yellow curve) show spectral features consistent with the CuO phase. After electrochemical reduction via cyclic voltammetry (red curve), the spectrum changes to reflect metallic Cu nanoparticles with a small peak around 650 nm attributable to the surface plasmon resonance of metallic Cu nanoparticles.

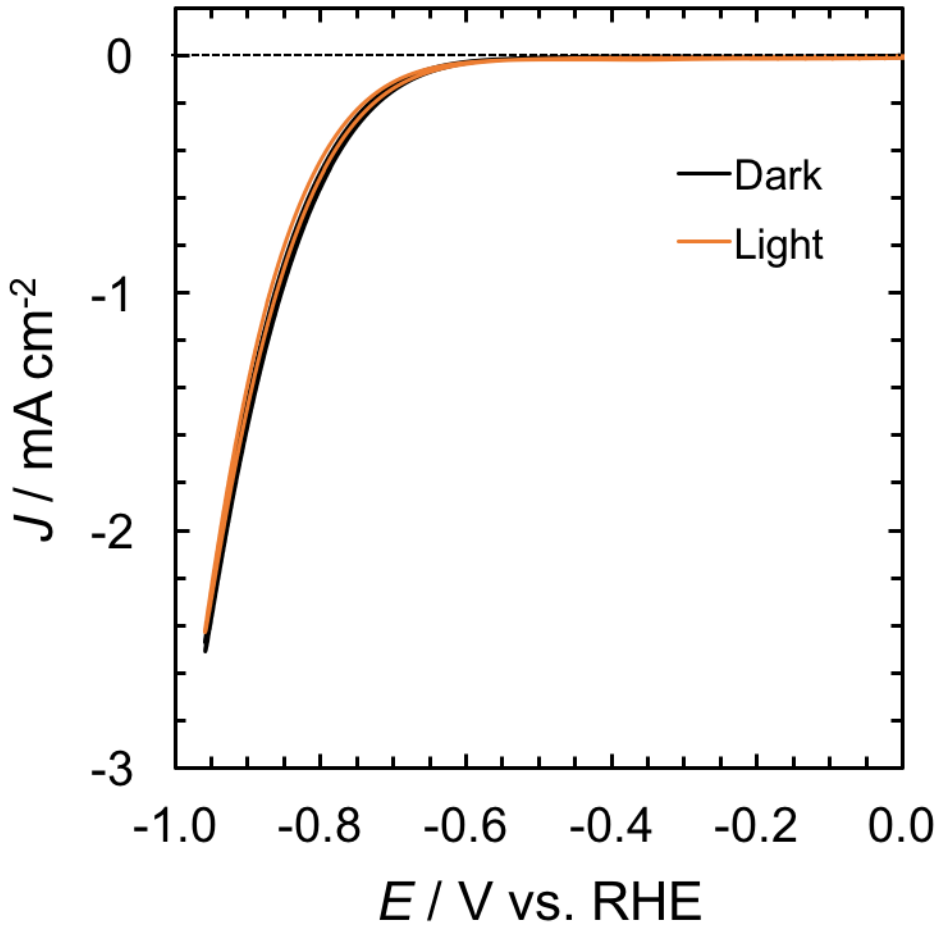

Figure S4. Cyclic voltammetry of bare p-NiO cathodes under dark (black curve) and visible light (orange curve) showing that bare p-NiO film exhibits no measureable light response across the potential sweep. This observation is consistent with the large band gap of p-NiO (see Figure S1d). Therefore, all visible-light responses observed from plasmonic Cu/p-NiO photocathodes can be unambiguously assigned to hot-hole injection from Cu to the valence band of p-NiO upon optical excitation of the Cu nanoparticles.

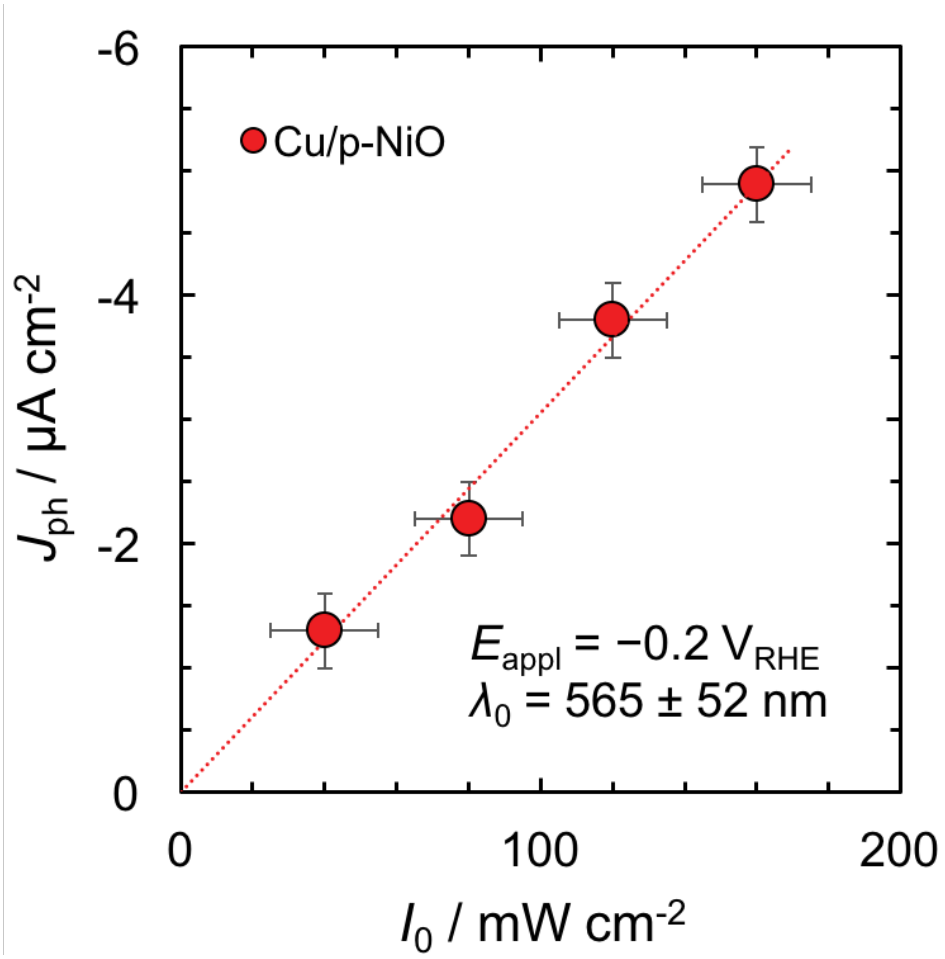

Figure S5. Power-dependence of the photocurrent $J_{ph}(I_0)$ obtained from the plasmonic Cu/p-NiO photocathode under visible-light irradiation (λ = 565 ± 52 nm) while potentiostatically poised at an applied potential of E_{appl} = −0.2 V_{RHE}.

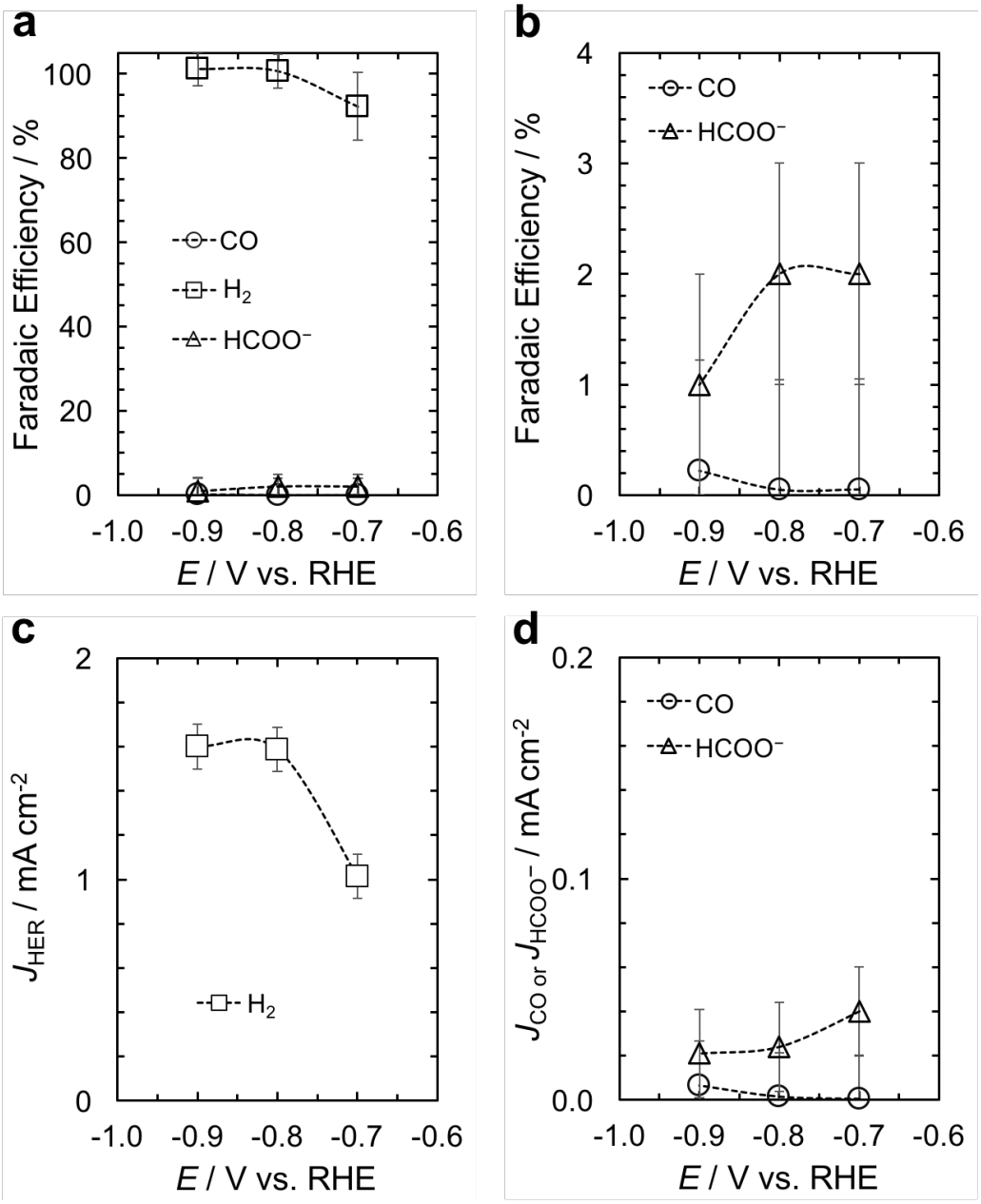

Figure S6. CO_2 reduction with bare p-NiO cathodes under dark conditions. (**a**-**b**) Faradaic efficiency for H_2 (squares), CO (circles), and $HCOO^-$ (triangles) with (**c**-**d**) corresponding partial current density *J* for the hydrogen evolution reaction (J_{HER}, squares), carbon monoxide (J_{CO}, circles), and formate (J_{HCOO-}, triangles). Electrolysis was performed under dark conditions in a CO_2-saturated 50 mM K_2CO_3 electrolyte. The device was held potentiostatically at each applied potential for 2 h while the gas products were sampled every 15 min and analyzed by gas chromatography. Liquid products were collected and analyzed by HPLC at the end of each run. Each data point represents the average of three independent trials and the error bar indicates the standard deviation.

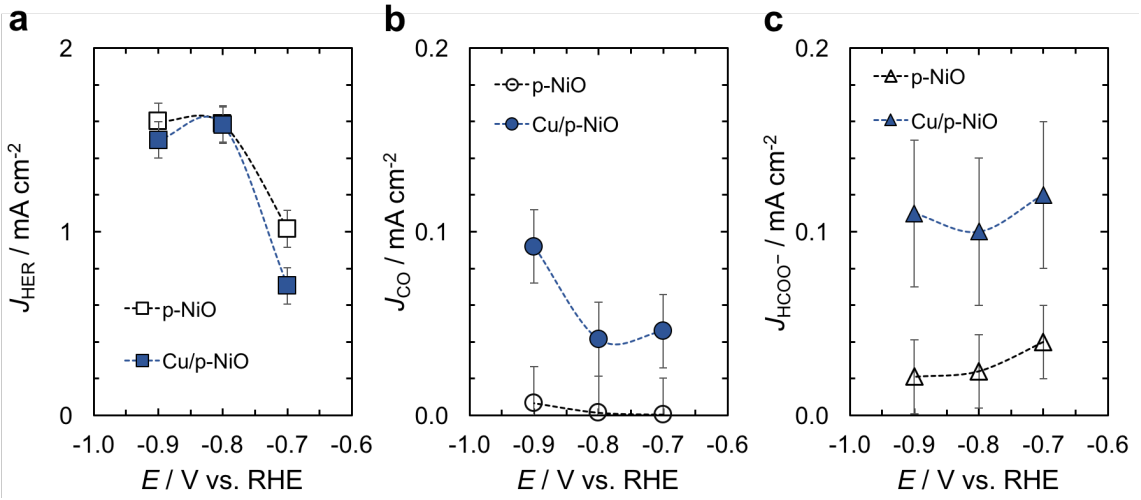

Figure S7. Comparison of the partial current densities (*J*) obtained from bare p-NiO (open data points) and Cu/p-NiO cathodes (filled data points) under dark conditions. (**a**) Partial current density for the hydrogen evolution reaction (J_{HER}) from p-NiO (open squares) relative to Cu/p-NiO (filled squares). (**b**) Partial current density for carbon monoxide (J_{CO}) from p-NiO (open circles) relative to Cu/p-NiO (filled circles). (**c**) Partial current density for formate (J_{HCOO^-}) from p-NiO (open triangles) relative to Cu/p-NiO (filled triangles). Each data point represents the average of three independent trials and the error bar indicates the standard deviation. We observed a significant increase in the partial current densities for CO_2 reduction products CO and $HCOO^-$ with the addition of Cu nanoparticles, while almost no change in the amount of H_2 that was evolved. We therefore attribute the significant amount of H_2 that is evolved from the plasmonic Cu/p-NiO device to the activity of the underlying p-NiO film, which almost exclusively produces H_2 under CO_2 reduction conditions (Figure S6).

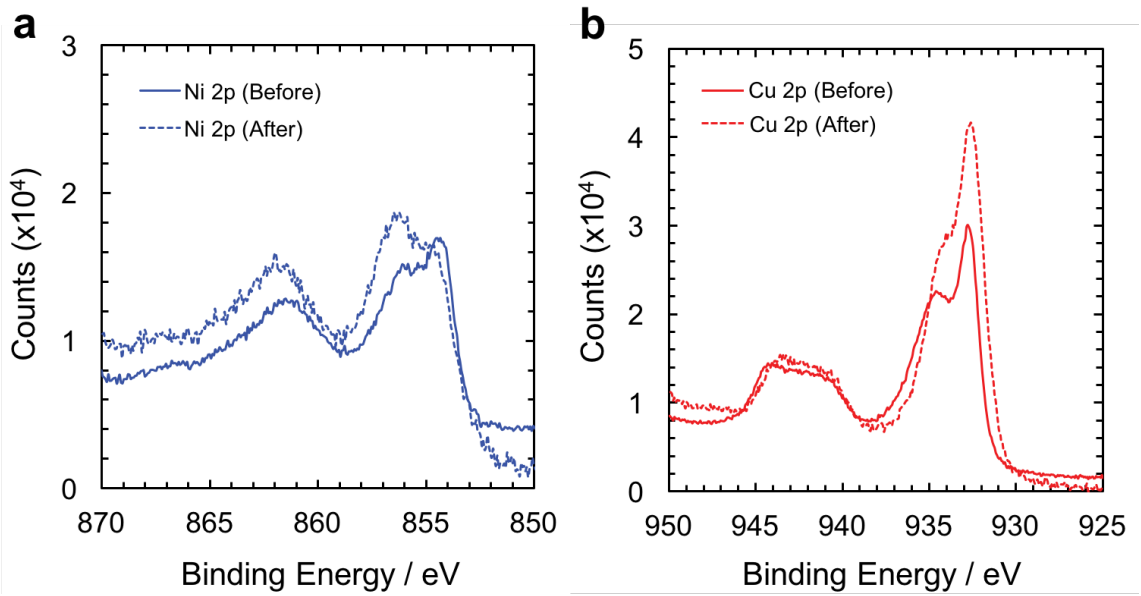

Figure S8. X-ray photoelectron spectroscopy high-resolution scans of **(a)** Ni 2p region and **(b)** Cu 2p region from the Cu/p-NiO photocathodes before (solid curves) and after (dashed curves) electrocatalysis. Despite some slight changes in relative peak ratio after electrocatalysis, these spectra show very similar characteristic binding energies and satellite features indicative of NiO and CuO, respectively.

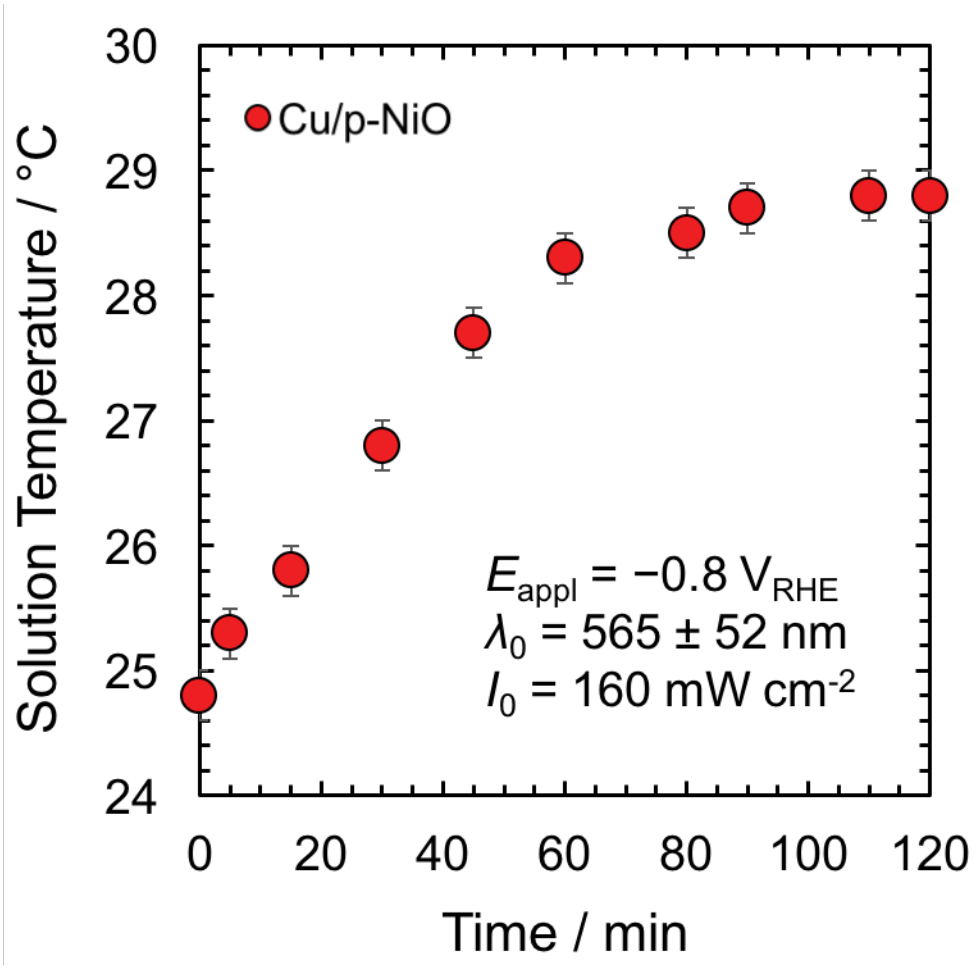

Figure S9. Plot of solution temperature over time during optical excitation of Cu/p-NiO photocathodes with a high-power LED. The solution temperature was recorded with a thermocouple immersed in the electrolyte of the specially-designed[2] photoelectrochemical cell, situated near the working electrode in the cell.

Supporting Information References

(1) Thimsen, E.; Martinson, A. B. F.; Elam, J. W.; Pellin, M. J. *J. Phys. Chem. C* **2012**, *116*, 16830-16840.

(2) Corson, E. R.; Creel, E. B.; Kim, Y.; Urban, J. J.; Kostecki, R.; McCloskey, B. D. *Rev. Sci. Instrum.* **2018**, *89*, 055112.